Lecture 25.
Wednesday 3rd June, 2020.
Compiled: Wednesday 10th June, 2020.

0.1 Higgs boson and properties

0.1.1 Expected properties of the Higgs boson

Now we look into the more specific properties of the Higgs field as predicted by the Standard Model. The Higgs field of the Standard Model contains only 4 degrees of freedom. We saw that 3 of these are Goldstone bosons that are eaten as the W and Z bosons obtain mass. What remains is only 1 dynamical field, the Higgs field $h(x)$. In the Standard Model Lagrangian $h(x)$ always appears together with the Higgs field vacuum expectation value v. Then the couplings of the Higgs boson are generated by the replacement:

$$v \longrightarrow v + h(x) \tag{1}$$

The couplings of h are then associated with the Standard Model mass terms. The Higgs interaction terms in the Standard Model Lagrangian are:

$$\begin{aligned}\Delta\mathcal{L} = &-\sum_f m_f \bar{f} f \frac{h(x)}{v} + 2m_W^2 W_\mu^+ W^{-\mu}\frac{h(x)}{v} \\ &+ \frac{2}{2} m_Z^2 Z_\mu Z^\mu \frac{h(x)}{v} - 3m_h^2 \frac{h(x)}{v} + \mathcal{O}(h^4)\end{aligned} \tag{2}$$

These terms are all P and C conserving, so the Higgs boson is a spin-0 particle with $P = +1$. It is possible to find that v has the value:

$$v = 246 \text{ GeV} \tag{3}$$

So all of the couplings of the Higgs boson are highly suppressed, except for the couplings to W, Z, and t. More general models of $SU(2) \times U(1)$ symmetry breaking also have this problem. Either W, Z, or t must be involved in the relevant processes, or the expected rates of Higgs boson processes are extremely small.
We will now discuss the processes that we can use to observe the Higgs boson. We must discuss both the production and decay processes. We will start with the decays. If m_h were greater than $2m_W$ and $2m_Z$, the dominant decays would be the decays to these particles:

$$h \longrightarrow W^+W^- \tag{4}$$
$$h \longrightarrow ZZ \tag{5}$$

These decays have been searched for at the LHC, but the only result has been to put strong limits on the production cross sections. Thus, the mass of the Higgs boson must be below the threshold for decay into WW.
In this case, the Higgs boson would decay dominantly into the next lightest Standard Model particle, the b quark. It is not so difficult to work out the decay rate for Higgs boson decay to $b\bar{b}$. The result is:

$$\Gamma(h \to b\bar{b}) = 3\frac{\alpha_w}{8} m_h \frac{m_b^2}{m_W^2}\left(1 - \frac{4m_b^2}{m_h^2}\right)^{\frac{3}{2}} \tag{6}$$

The quark mass should be evaluated at $Q \approx m_h$, giving a value of about 3 GeV for m_b. Then, for a Higgs boson of mass 125 GeV, we find:

$$\Gamma(h \to b\bar{b}) \approx 2 \text{ MeV} \tag{7}$$

Recall that the width of the Z boson is about 2.5 GeV, a thousand times larger. So the Higgs boson is very narrow, so narrow that it will be difficult to measure the width directly. Other relevant decays to quarks and leptons

$$h \longrightarrow \tau^+\tau^- \tag{8}$$

$$h \longrightarrow c\bar{c} \tag{9}$$

give decay rates about 10 times smaller than the decay rate to $b\bar{b}$.
Because the decay to $b\bar{b}$ is so highly suppressed, higher-order decay processes can compete with it. First, although $h \to WW, ZZ$ are forbidden, it is possible that the Higgs boson can decay through a diagram in which an off-mass-shell W and Z appears as a resonance, as in Figure 1.

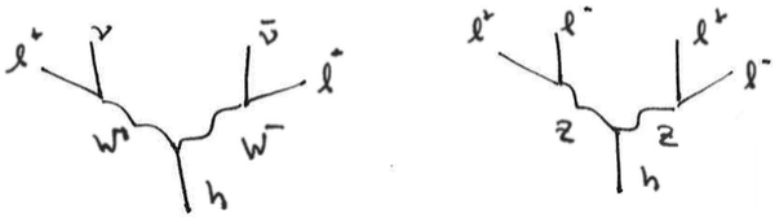

Figure 1: Decay of the Higgs boson to off-mass-shell W and Z pairs.

These decays are called $h \to WW^*$ and $h \to ZZ^*$. The suppression from multi-body phase space and the tail of the Breit-Wigner distribution is comparable to the suppression seen above from the small size of $(m_b/v)^2$.
It is also possible for a Higgs boson to decay through higher-order processes involving virtual top quarks or W bosons. This gives decays to two gluons, as in Figure 2, to two photons, as in Figure 3, and to γZ.

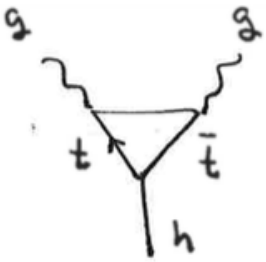

Figure 2: Higgs decay to two gluons.

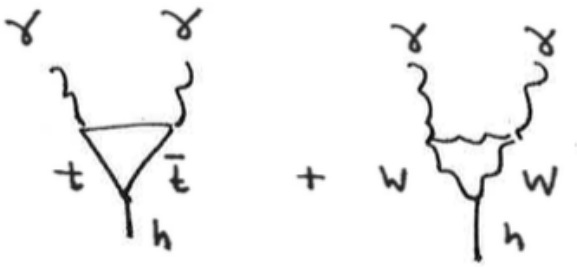

Figure 3: Higgs decay to two photons.

For a 125 GeV Higgs boson, the rate for $h \to 2g$ is comparable to the rate for $h \to \tau^+\tau^-$ and $h \to WW^*$. The rate for $h \to \gamma\gamma$ is about a factor of 50 smaller.
A full set of predictions for the branching ratios of the Higgs boson within the Standard Model, as a function of the Higgs boson mass, is showed in Figure 4. These

predictions of the Standard Model do not involve any parameters other than those that we have already discussed. Thus, the predictions can be highly precise. Does nature agree with these results?

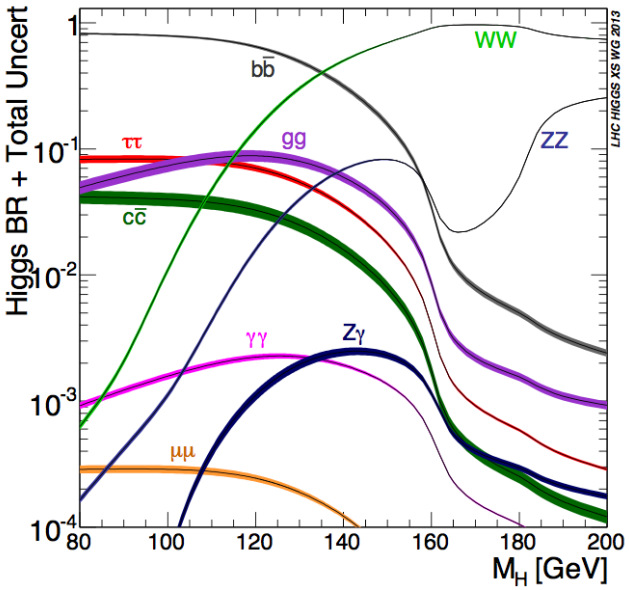

Figure 4: ranching ratios for decays of the Higgs boson as a function of the Higgs boson mass, predicted in the Standard Model.

0.1.2 Measurements of Higgs boson properties at the LHC

Reversing the decay processes, we find processes for producing the Higgs bosons in high energy collisions. An obvious production process is:

$$b\bar{b} \longrightarrow h \tag{10}$$

However, at the LHC, the cross section for this process is multiplied by the very small b quark pdf in the proton. The most promising production mode at the LHC turns out to be $gg \to h$, or **gluon-gluon fusion**, represented in the diagram in Figure 5, using the Higgs coupling to two gluons showed above.

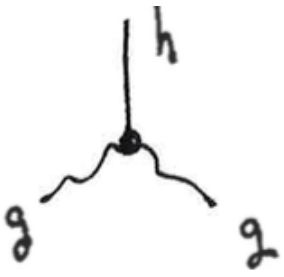

Figure 5: Gluon-gluon fusion diagram.

The intrinsic strength of the interaction is smaller, but the initial gluons can be taken from the very large gluon pdf in the proton. At the 13 TeV LHC, a gluon momentum fraction of $x \sim 0.01$ is all that is required.
Another important production process is **vector boson fusion**, represented in Figure 6, in which high-x quarks in the proton create virtual W or Z bosons that then combine to produce a Higgs boson.

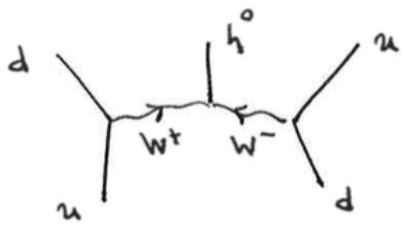

Figure 6: Vector boson fusion diagram.

Notice that this process results in a Higgs boson and two high-energy jets emitted in the forward direction. The presence of the forward jets can then be used to enhance the Higgs boson signal.
A third important reaction is production of a Higgs boson in association with a W or Z boson. This process can be imagined as $q\bar{q}$ annihilation to the weak boson followed by radiation of a Higgs boson using the relatively large Higgs coupling to these particles. This process is represented in Figure 7.

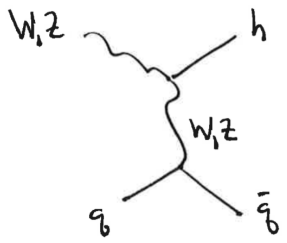

Figure 7: Diagram of production of h in association with W and Z bosons.

Predictions for these and other Higgs boson production processes at the LHC are showed in Figure 8.

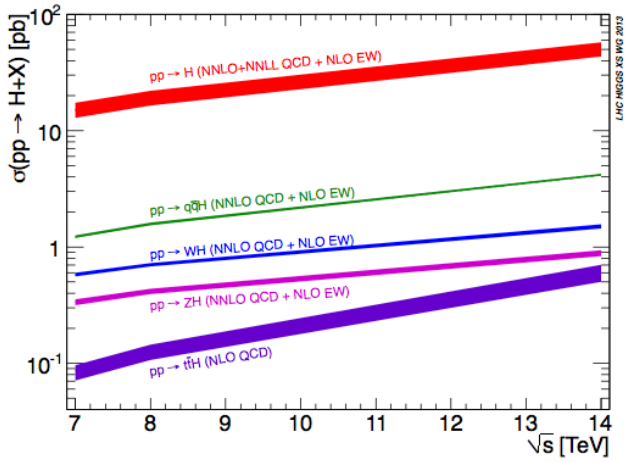

Figure 8: Cross sections for production of the Higgs boson at the LHC as a function of center of mass energy, predicted in the Standard Model.

For $m_h = 125$ GeV and an LHC center of mass energy of 13 TeV, the cross sections are:

$$\sigma(pp \to gg \to h) = 50 \text{ pb} \tag{11}$$
$$\sigma(pp \to WW \to h) = 4 \text{ pb} \tag{12}$$
$$\sigma(pp \to Wh, Zh) = 2 \text{ pb} \tag{13}$$

These results should be compared with the proton-proton total cross section of about 100 mb, which is higher by a factor of $2 \cdot 10^9$.
At the LHC, we do not observe the total rate for Higgs production. Rather, we reconstruct the Higgs boson in a particular decay mode. The quantity that we measure has the form of a cross section times branching ratio, $\sigma \cdot \mathrm{BR}$, for example:

$$\sigma(gg \to h) \cdot \mathrm{BR}(h \to b\bar{b}) \tag{14}$$

In general, a separate selection must be used for each separate decay mode.
Unfortunately, many of the most important Higgs boson decay modes are difficult to observe at the LHC. For example, the process:

$$gg \to h \to b\bar{b} \tag{15}$$

results in two b quark jets. However, the QCD process:

$$gg \to b\bar{b} \tag{16}$$

also produces pairs of b quark jets, with jet pair masses at and above the Higgs boson mass, at a rate about a million times greater. In the decays $h \to WW^*$ and $h \to ZZ^*$, events with hadronic decays of the W and Z are difficult to recognize for the same reason.
To discover the Higgs boson, the ATLAS and CMS experiments at the LHC concentrated their efforts on decay modes of the Higgs boson to photons and leptons in which all final state particle would be visible. These modes are:

$$h \longrightarrow \gamma\gamma \qquad \mathrm{BR} = 0.23\% \tag{17}$$

$$h \longrightarrow ZZ^* \longrightarrow 4\ell \qquad \mathrm{BR} = 0.016\% \tag{18}$$

In all, Higgs boson production and decay into these modes occurs in about 1 in $2 \cdot 10^{12}$ pp collisions. It was quite a feat to collect such events in the presence of enormous numbers of more ordinary LHC collisions. By collecting a very large data set, the LHC experiments were able to identify the Higgs boson in these channels. Figure 9 shows a candidate $pp \to h \to \gamma\gamma$ event from CMS. Figure 10 shows the distribution of $pp \to \gamma\gamma$ events found by CMS as of June 2012 as a function of the invariant mass of the $\gamma\gamma$ pair. There is a clear resonance on the expected smooth background at a mass of about 125 GeV. Figure 11 shows a candidate $pp \to h \to e^+e^-\mu^+\mu^-$ event collected by the ATLAS experiment. Figure 12 shows the 4-lepton events seen by the ATLAS experiment as of June 2012, plotted as a function of the 4-lepton invariant mass. A signficant resonance signal is seen at the same mass of 125 GeV. On July 4, 2012, both experiments showed significant signals in both of these channels, presenting strong evidence for the appearance of this particle.
With the new particle identified, we can ask whether it indeed has the properties expected for the Higgs boson. First, is it a particle with $J^P = 0^+$, as the Standard Model predicts? If the new resonance decays to $\gamma\gamma$, it cannot be a particle of spin 1. However, the possibilities of spin greater than 1, and of $P = -1$, would still be open. These hypotheses can be addressed using $h \to ZZ^* \to 4$ leptons events. The relative orientations of the leptons in these events give information on the polarizations of the Z bosons in $h \to ZZ^*$. Also, they allow tests of whether the particle production and decay is independent of orientation, as would be expected for a spin-0 particle. Figure 13 shows tests of the various spin and parity hypotheses relative to the hypothesis of $J^P = 0^+$. In all cases, the 0^+ hypothesis is favored. In most cases, this hypothesis is strongly favored already with this sample of about 25 events.

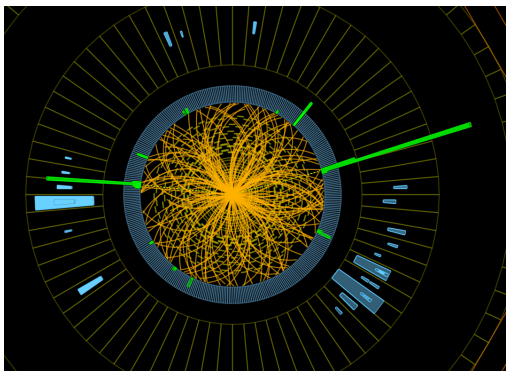

Figure 9: Candidate $pp \to h \to \gamma\gamma$ event observed by the CMS experiment at the LHC.

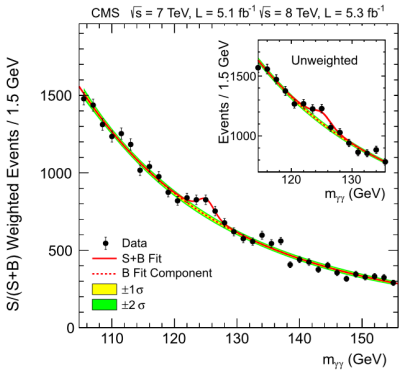

Figure 10: Mass distribution of γ pairs measured by the CMS experiment at the LHC. In main plot, events more likely to be well-reconstructed $pp \to \gamma\gamma$ events are given higher weight.

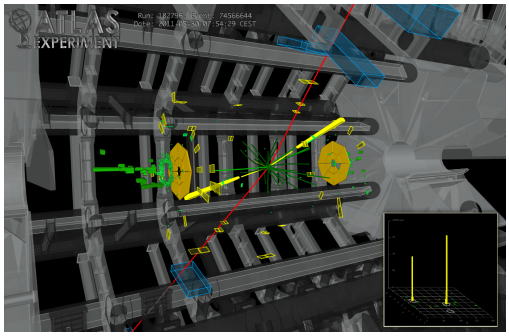

Figure 11: Candidate $pp \to h \to e^+e^-\mu^+\mu^-$ event observed by the ATLAS experiment at the LHC.

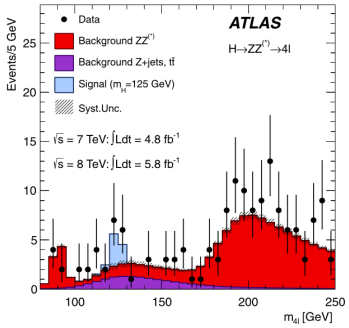

Figure 12: Mass distribution in four-lepton events measured by the ATLAS experiment at the LHC.

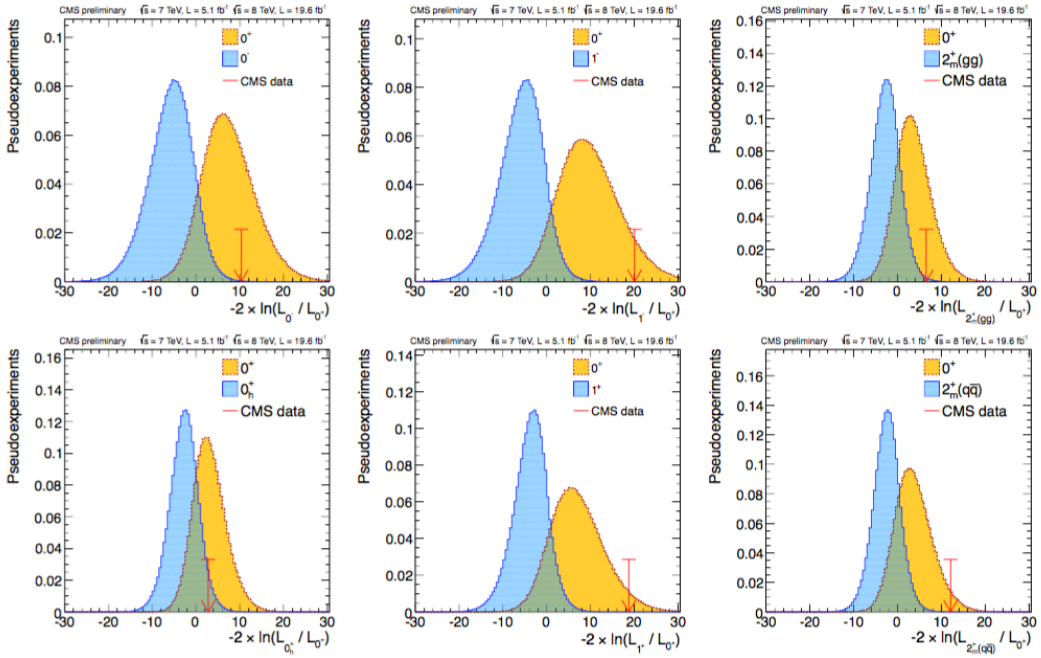

Figure 13: Comparison of hypotheses for the spin and parity of the 125 GeV resonance from event distributions in $h \to 4\ell$. What is shown in each plot is the distribution of a test statistic expected for the Standard Model 0^+ hypothesis (yellow) and for an alternative hypothesis (blue). The arrow shows the value of the test statistic given by the data.